

Investigation of Phase Delay Dispersion of the Meander Lines using Hybrid Technique

Antanas Gurskas¹, Audrius Krukoniš¹, Vytautas Urbanavicius¹

¹Department of Electronic Systems, Vilnius Gediminas Technical University, Naugarduko St. 41–422, LT-03227 Vilnius, Lithuania
audrius.krukoniš@vgtu.lt

Abstract—Periodical slow-wave systems, for example helical or meander delay lines are dispersive. I. e. velocity of propagation of electromagnetic wave in such systems, or delay time of a signal in the correspondent line, depends on wave frequency. This fact reduces the bandwidth of such systems or lines, even if losses are totally absent in it. Delay dispersion of such systems at high frequencies can be explained by coupling of adjacent conductive strips and the frequency properties of the dielectric materials. However, the dispersion at low frequencies, hardly investigated until now. The sources of phase delay dispersion of the meander microstrip delay lines and some other slow-wave systems at low frequency range are investigated in this paper. To study the dispersion of delay systems mathematical and computer modelling, and experimental measurements were used.

Index Terms—Microwave circuits, delay effects, dispersion, time measurement.

I. INTRODUCTION

Slow-wave systems are widely used in RF and microwave electronics. Examples include, but are not limited to: travelling-wave tubes for velocity matching of flight of the electron beam and electromagnetic waves [1], in analog signal processing systems to separate certain components of the frequency spectrum [2], in antenna arrays to form a predetermined pattern and control it [3] as well as delay lines (DL) for signals phase matching [4].

The phase nominal delay $t_{ph\ d}$ is one of the most important parameters in designing the DL, moreover, the nominal characteristic impedance Z_0 and bandwidth ΔF , which for electrodynamic lines starting at zero, are specified also.

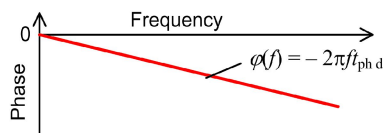


Fig. 1. Phase-frequency response of the non-dispersive delay line.

Mathematically, the frequency response of the phase delay of the DL is determined from its phase-frequency response (Fig. 1) according to the well-known formula [5]

$$t_{ph\ d}(f) = \frac{\phi(f)}{-360^\circ f}, \quad (1)$$

where ϕ is the phase difference between the input and the output waveforms of the DL at frequency f .

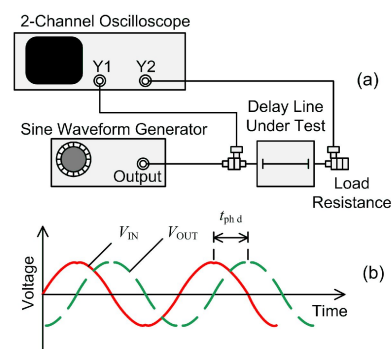


Fig. 2. The direct phase delay measurement technique: (a) scheme; (b) the voltage waveforms at the input and output of the delay line under test.

Practically the frequency response of the phase delay can be measured in different ways e.g.: directly, by measuring the phase time delay between the input and output waveforms by 2-channel oscilloscope (Fig. 2), by other direct technique using a vector network analyser (VNA) [5], or indirectly by using a scalar vector network analyser (SVA), also called a resonance measurement technique (Fig. 3).

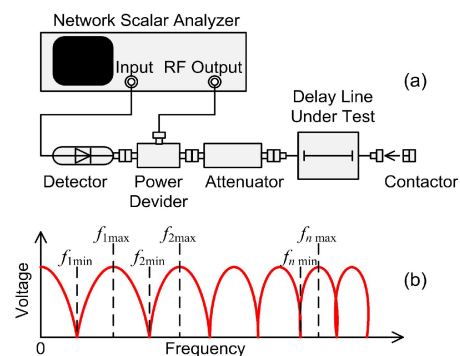


Fig. 3. The resonance phase delay measurement technique: (a) scheme; (b) the voltage waveform at the input of the delay line under test.

Using the resonance technique, when the end of the line is opened (load resistance is infinite), the phase delay is calculated according to this formula

$$t_{ph\ d}(f) = \frac{n_{max}}{2f_{n\ max}} = \frac{2n_{min} - 1}{4f_{n\ min}}, \quad (2)$$

where $n_{max/min}$ is the number of n -th maximum/minimum of the frequency response of the input voltage of the open-end

DL waveform; $f_{n \max/\min}$ is the corresponding frequency of n -th maximum/minimum. In the case of a short-circuited line (load resistance is zero) the phase delay is calculated by the slightly modified equation

$$t_{\text{ph d}}(f) = \frac{2n_{\max} - 1}{4f_{n \max}} = \frac{n_{\min}}{2f_{n \min}}. \quad (3)$$

Delay dispersion of periodic slow-wave systems at high frequencies has long been known and can be explained by coupling of adjacent conductive strips and the frequency properties of the dielectric materials. This kind dispersion is often used for practical purposes [6], [7]. It was observed however that measuring the phase delay $t_{\text{ph d}}(f)$ of the meander DL [8] in the given frequency band ΔF by the resonance technique, the delay at low frequencies often significantly higher than the values in the midrange [9]. This phenomenon, when increasing the wave frequency slow rate decreases, called anomalous dispersion. It is known that the phase delay of the line depends on the dielectric constant of the medium in which the wave propagates. However, at lower frequencies, the dielectric constant changes in a very small range and can not cause such a large increase in phase delay. Initially, it has been suggested that such deviations caused by the specifics of the resonance technique and the periodic nature of the meander line structure, however, similar deviations were found in other works, where other methods of measurement and over slow-wave structure were used [10]–[13].

The deviations of the phase delay of the DL from the nominal value are investigated in this paper; various methods of modelling and measurements are used; the causes of the deviation at low frequencies are established. The paper is organized as follows. In Section II methods of calculating the phase frequency response of the DL (model based on the concept of an ideal transmission line, model based on the theory of two-port network, and the model, which combined S-matrix technique and the method of moments) will be pointed out. Several interesting calculation and simulation cases with experimental results are presented in Section III with a conclusion given in Section IV.

II. MATHEMATICAL MODELS OF DELAY LINES

Four models of the delay lines, allowing to calculate the frequency response of the phase delay, described in this section.

A. Model Based on the Concept of an Ideal Transmission Line

The ideal transmission line length of l has no losses, and can be regarded as DL with a linear phase-frequency response that defines this expression

$$\{ (f) = -2 f t_{\text{ph d}}, \quad (4)$$

where $t_{\text{ph d}}$ is the nominal delay of the line. The input impedance Z_{IN} of such line loaded on resistance Z_L is calculated according to the formula [14]

$$Z_{\text{IN}} = Z_0 \frac{Z_L + jZ_0 \tan sl}{Z_0 + jZ_L \tan sl}, \quad (5)$$

where $s = 2\pi f/v_{\text{ph}}$ is the phase coefficient of the wave propagated in the line with phase velocity v_{ph} , Z_0 is characteristic impedance of the line, $j = -1^{1/2}$ is the imaginary unit.

The complex frequency response of such ideal line connected between the source of oscillations with internal impedance $Z_S = Z_L$ is calculated by the formula

$$\underline{K} = \frac{V_{\text{OUT}}}{V_{\text{IN}}} = \frac{Z_L}{Z_0} \left[\frac{Z_0 Z_L (1 + \tan^2 sl)}{Z_L^2 + Z_0^2 \tan^2 sl} - j \frac{\tan sl (Z_0^2 - Z_L^2)}{Z_L^2 + Z_0^2 \tan^2 sl} \right] e^{sl}, \quad (6)$$

where V_{OUT} and V_{IN} are the phasors of the output and the input voltage of the line respectively. A phase-frequency response of this line is determined by this equation

$$\{ (f) = - \left[\tan^{-1} \left(\frac{Z_0^2 - Z_L^2}{Z_0 Z_L} \frac{\tan sl}{1 + \tan^2 sl} \right) + sl \right]. \quad (7)$$

B. Model Based on the Theory of Two-Port Network

The ideal DL can also be seen as two-port network, which complex frequency response is determined by this equation [15]

$$\underline{K} = \frac{Z_L}{\underline{A}Z_L + \underline{B} + \underline{C}Z_S Z_L + \underline{D}Z_S}, \quad (8)$$

where Z_S is the internal impedance of the source of oscillations connected to the input of the two-port network, \underline{A} , \underline{B} , \underline{C} and \underline{D} are complex matrix elements

$$\begin{bmatrix} \underline{A} & \underline{B} \\ \underline{C} & \underline{D} \end{bmatrix} = \begin{bmatrix} \cos sl & jZ_0 \sin sl \\ j\frac{1}{Z_0} \sin sl & \cos sl \end{bmatrix}. \quad (9)$$

The phase-frequency response of such two-port network is determined by the equation

$$\{ (f) = - \tan^{-1} \left(\frac{Z_0 + Z_S Z_L / Z_0}{Z_S + Z_L} \tan sl \right). \quad (10)$$

C. Model Based on the S-Matrix Technique

The meander DL (Fig. 4) is calculated using S-matrix technique [15]. The matter of the technique is based on the calculation of final meander DL S-matrix, conversion it to \underline{A} , \underline{B} , \underline{C} , \underline{D} matrix and finding of phase delay frequency response according to formulas (8)–(10). Final meander DL S-matrix is determining from detailed meander DL S-matrix which is build filling the main and two adjacent diagonals by primitive four elements S-sub matrices. The main diagonal sub-matrices corresponds to wave travelling along meander strips, while upper and lower diagonals matrices corresponds to coupling properties between neighbour meander strips. Elements of the main S-matrix are calculated from parameters of the matrix \mathbf{b}

$$\mathbf{b} = (-\mathbf{S}_d)^{-1} \mathbf{c}, \quad (11)$$

where X is reflection coefficient matrix, \mathbf{c} is excitation matrix and \mathbf{S}_d is meander DL detailed S-matrix. Primitive sub-matrix elements in the main and adjacent diagonals of detailed meander DL S-matrix is determined according to empirical formulas [15].

D. Hybrid Model of the Meander Delay Line

Hybrid model of meander microstrip DL is based on the same S-matrix technique. The difference is only in determining of primitive S-sub matrices in the main and adjacent diagonals [16]. In this case method of moments (MoM) for calculation of the wave impedance and effective permittivity in case of odd- and even- excitation Z_e , Z_o , v_e and v_o is used. The benefit of this model is that the MoM estimates meander microstrip DL heterogeneity along the meander line (L in Fig. 4). It should also be noted that this model allows to imitate both the direct measurement of the phase delay (using a phase-frequency response and (1)), and an indirect (resonance) measurement using (2) and (3).

III. INVESTIGATION OF PHASE DELAY DISPERSION

To determine the causes of phase delay deviation from its nominal, models of an ideal DL, models of the microstrip meander DL (see Section II) and the real prototype of the microstrip meander DL were investigated.

Ideal DL parameters were chosen as follows: nominal phase delay $t_{phd} = 5$ ns, three values of characteristic impedance: 1) $Z_0 = 50 \Omega$, 2) $Z_0 = 75 \Omega$ and 3) $Z_0 = 37.5 \Omega$. Such selected impedance values correspond to $\pm 33\%$ deviation of the investigated line characteristic impedance from 50Ω impedance of the signal path, which includes the studied line.

The design of the prototype of the microstrip meander DL and the design parameters are shown in Fig. 4.

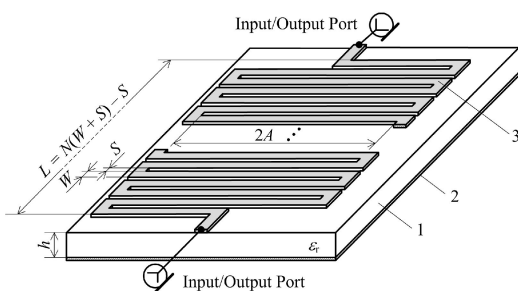


Fig. 4. The prototype of the microstrip meander delay line, where 1 is the dielectric substrate, 2 is a reference conductor, 3 is the meander-shaped microstrip, $h = 0.5$ mm, $v_r = 5.0$, $W = 0.64$ mm, $S = 0.35$ mm, $2A = 18.36$ mm, $N = 55$, $L = 54.1$ mm.

Magnitude of the deviation of the phase delay will assess the relative value

$$u_{t_{phd}} = \left[\frac{t_{phd}^{(Z_0)} - t_{phd}^{(50)}}{t_{phd}^{(50)}} \right] 100\%, \quad (11)$$

where $t_{phd}^{(Z_0)}$ is the phase delay of line of characteristic impedance Z_0 50Ω , $t_{phd}^{(50)}$ is the phase delay of line of

impedance $Z_0 = 50 \Omega$.

Magnitude of the deviation of line characteristic impedance will assess the relative value

$$u_{Z_0} = \left[\frac{(Z_0 - 50 \Omega)}{50 \Omega} \right] 100\%, \quad (12)$$

where Z_0 is the characteristic impedance of DL under test.

A. Phase Delay of the Ideal Delay Lines

The phase delay frequency response of the ideal line, calculated in accordance with the mathematical models described in Section II A, B and C, are shown in Fig. 5. Deviations of phase delay at low frequencies of the DL mathematical models are presented in Table I.

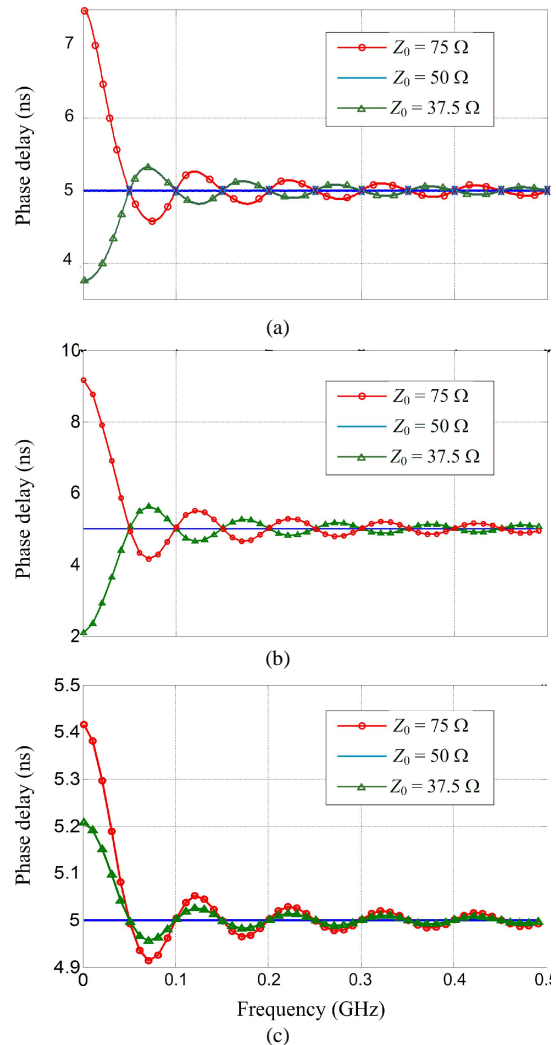


Fig. 5. Calculated phase delay frequency response of the ideal transmission line having various characteristic impedance Z_0 and integrated in 50Ω signal path. Mathematical models: (a) “S-matrices”; (b) “transmission line”; (c) “two-port network”.

It can be seen in Fig. 5 that the deviation of the phase delay of lines, which correspond to models of “S-matrices” (Fig. 5(a)) and “transmission line” (Fig. 5(b)), at a frequency close to zero, from the delay of the matched line, depends on the deviation of line characteristic impedance on the impedance of the signal path. Moreover, in the case of “S-matrices” model, delay variation $u_{t_{phd}}$ is directly proportional to the deviation of the impedance u_{Z_0} and is equal to $\pm 33\%$. And in the case of the “transmission line”

model, this proportion is not met and similar deviations are $U_{r_{ph d}} = +84\%$ and $U_{r_{ph d}} = -40\%$ respectively.

Despite such large deviations of the phase delay at low frequencies in reality it is a very small part of the period of the transmitted signal, and it does not matter phase distortions. For example, when delay deviation is 84% at a frequency of 1 MHz (in our case 9.2 ns and 5.0 ns respectively, see Fig. 5(b)), a phase deviation is only equal to $2 \cdot \pi \cdot 4.2 \cdot 10^{-9} / 10^{-6} = 8.4 \cdot 10^{-3} \pi \text{ rad} \cong 0.026 \text{ rad} \cong 1.512^\circ$.

TABLE I. DEVIATION OF PHASE DELAY AT LOW FREQUENCIES OF THE DELAY LINE MATHEMATICAL MODELS.

Characteristic impedance deviation	Phase delay deviation calculated according to (11)		
	Mathematical models		
	“S-matrices”	“Transmission line”	“Two-port network”
$Z_0 = +33\%$	+33 %	+84 %	+8.4 %
$Z_0 = -33\%$	-33 %	-40 %	+4 %

It should be noted that the deviation of the phase delay of the “two-port network” model is positive even when the deviation of characteristic impedance is negative (Fig. 5(c)). Deviations of the phase delay here is nearly 10 times less than in the case of the “transmission line” model.

Frequency responses of the ideal lines phase delay were also simulated using SONNET[®] and CST Microwave Studio[®] software (Fig. 6). This can be seen here that the responses obtained using SONNET[®] simulator (Fig. 6(a)) are almost identical to the responses of the model “two-port network” (Fig. 5(c)), and in the case of the CST Microwave Studio[®] simulator (Fig. 6(b)) received several large deviations of the phase delay at low frequencies – 13% and 8% respectively.

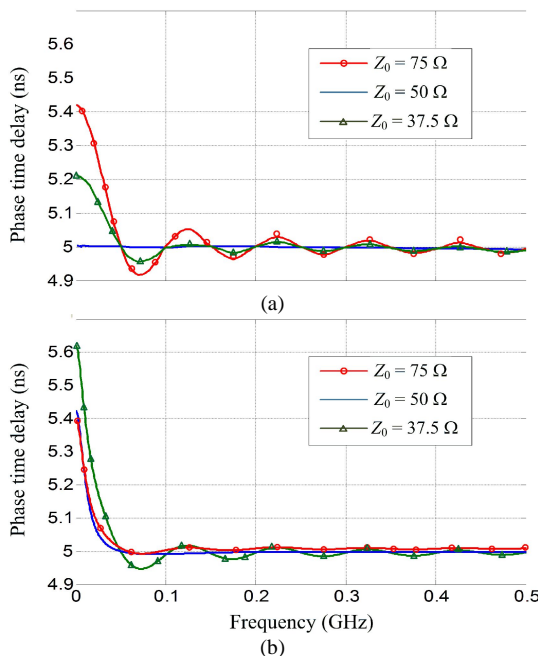


Fig. 6. Simulated phase delay frequency response of ideal transmission line having various characteristic impedance Z_0 and integrated in 50 Ω signal path. Simulation software: (a) SONNET[®]; (b) CST Microwave Studio Suit[®].

It should be noted that in all the frequency responses of the phase delay (Fig. 5 and Fig. 6) of mismatched lines ($Z_0 \neq 50 \Omega$) curves oscillations whose period corresponds to

the nominal delay $t_{ph d} = 5 \text{ ns}$ (i.e. $1/(t_{ph d}) = 1/(5 \cdot 10^{-9}) = 0.1 \text{ GHz}$) are visible.

B. Phase Delay of the Meander Delay Line Prototype

Experimental prototype of the microstrip meander DL (Fig. 4) was manufactured and measured (Fig. 7) to check the adequacy of the mathematical model of the DL based on the hybrid method (Section II, D).

The measurements of the prototype were carried out in three stages:

1. Using the VNA HP8753E the phase-frequency response of the prototype was directly measured and according to (1) its phase delay was calculated (Fig. 8(a));

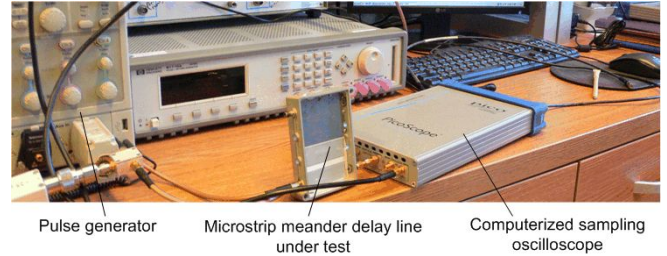


Fig. 7. Photo of the experimental setup for the time domain measurement.

2. Using the SVA measurement systems, which consists of HP182T, HP8350A, HP11666A, HP83592A devices, and (2) and (3), the phase delay was measured indirectly by the resonance method (Fig. 8(b));
3. Using sampling oscilloscope PicoScope 9300 time delay between the leading edges of the rectangular pulse at the input and output lines was measured (Fig. 9).

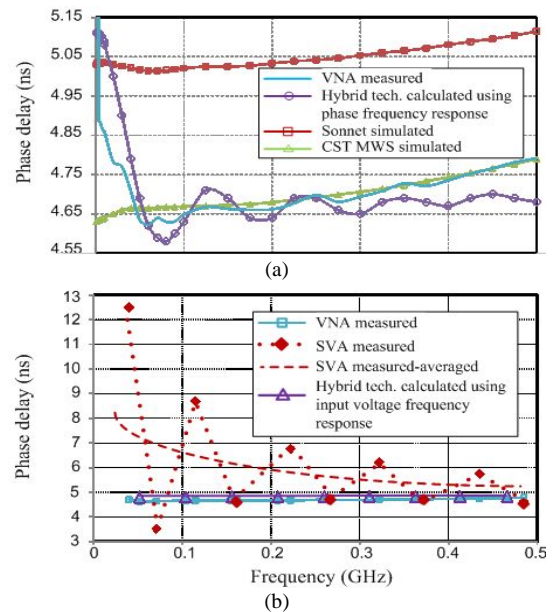


Fig. 8. Comparison of measured, simulated and calculated phase delay frequency response of the meander delay line: (a) direct measurement using VNA, calculation using the hybrid method and simulation; (b) indirect measurement using SVA (resonance technique), calculation using a hybrid method that simulates resonance measurement technique.

Direct measurements (Fig. 8(a)) showed that the phase delay of the meander DL calculated using the proposed hybrid technique differs from the measured values no more than 3% at all frequencies above 30 MHz. For comparison, the curves obtained by simulation are shown in Fig. 8(a) as well. It also can be seen that the hybrid technique detects

anomalous dispersion at low frequencies.

Indirect measurement using the resonance technique yields only the individual values of the frequency response of the phase delay (Fig. 8(b)). Also this technique is very sensitive to mismatched signal path and to losses in the line under test. As a result, the measurement of the phase delay gives a very sloping curve. Despite this, the difference between the values of phase delay calculated using the hybrid technique, and the averaged values of the resonance measurement does not exceed 18 % at a frequency of 0.2 GHz, and at 0.5 GHz it is reduced even up to 9 %.

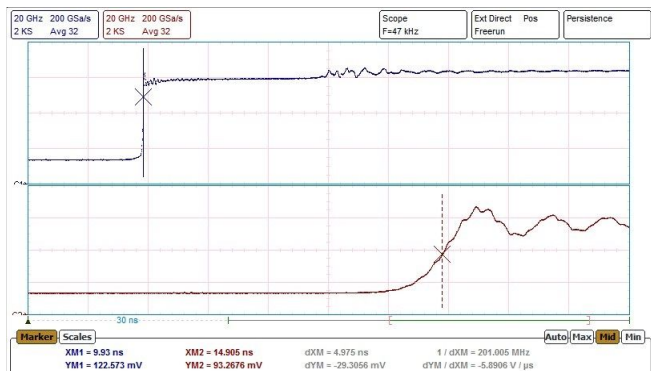


Fig. 9. Measured transients on the input (top) and output (bottom) of the microstrip meander delay line. Measured delay parameters, shown on the bottom are: time marker “XM1” – 9.93 ns, time marker “XM2” – 14.905 ns and time marker difference “dXM” – 4.975 ns.

The measurements in the time domain are sufficient to objectively assess the investigated DL. In this case, the delay time between the leading edges of square pulses at the input and output of the meander DL (Fig. 9) is equal to 4.975 ns and only 7 % higher than the value obtained by direct measurement using the VNA (Fig. 8(b)).

IV. CONCLUSIONS

Almost all delay systems with periodical structure inherent dependence of the phase delay of the frequency, especially at high frequencies, where the slowdown factor is increasing. This phenomenon is known as the normal dispersion.

Some delay systems at lower frequencies also shown anomalous dispersion, i.e. in this case retardation decreases with increasing frequency.

In this work it was established that the cause of dispersion at low frequencies is the mismatch of the characteristic impedance of delay system under test.

It was found that despite significant absolute values of dispersion at low frequencies, this corresponds to vanishingly small values of the period of the signal being slowed down and, in fact, not a phase distortion.

Hybrid technique of analysis of meander delay lines based on a combination of the MoM and S-matrices technique is a very effective tool for studying periodic delay systems. Frequency responses (several hundred points) computation time using the hybrid technique is measured by few tens of seconds, and the difference between the calculated and measured values often does not exceed 5 %.

Some our offered mathematical models of the delay line demonstrated at low frequencies not only abnormal but normal dispersion also. Experimental research of such

systems prototypes is our task for the near future.

ACKNOWLEDGMENT

We are very grateful to JSCs ELMIKA, ELTESTA and GEOZONDAS for their help organizing and conducting experimental measurements. We are also grateful to Prof Romanas Martavicius for fruitful discussions and useful comments.

REFERENCES

- [1] L. Xu, Z.-H. Yang, J.-Q. Li, B. Li, “A 3-D finite-element Eigenvalue analysis of slow-wave structures of traveling-wave tubes without matching meshes”, *IEEE Trans. On Microwave Theory and Techniques*, vol. 61, pp. 3524–3528, 2013. [Online]. Available: <http://dx.doi.org/10.1109/TMTT.2013.2277996>
- [2] Y. Horii, S. Gupta, B. Nikfal, C. Caloz, “A high slow-wave factor microstrip structure with simple design multilayer broadside-coupled dispersive delay line structures for analog signal processing”, *IEEE Microwave and Wireless Components Letters*, vol. 22, pp. 1–3, 2012. [Online]. Available: <http://dx.doi.org/10.1109/LMWC.2011.2176476>
- [3] S.-S. Zhong, X.-X. Yang, S.-C. Gao, “Polarization-Agile microstrip antenna array using a single phase-shift circuit”, *IEEE Trans. On Antennas and Propagation*, vol. 52, pp. 84–87, 2004. [Online]. Available: <http://dx.doi.org/10.1109/TAP.2003.820953>
- [4] Y. S. Wong, S. Y. Zheng, W. S. Chan, “Multi-way and poly-phase aligned feed-forward differential phase shifters”, *IEEE Trans. On Microwave Theory and Techniques*, vol. 62, pp. 1312–1321, 2014. [Online]. Available: <http://dx.doi.org/10.1109/TMTT.2014.2316745>
- [5] Group and Phase Delay Measurements with Vector Network Analyser ZVR. Application Note 1EZ35_1E, Rohde & Schwarz GmbH & Co. KG, Munchen, 1996, pp. 2–4.
- [6] G. Chaudhary, Y. Jeong, “Multi- low signal-attenuation negative group-delay network topologies using coupled lines”, *IEEE Trans. On Microwave Theory and Techniques*, vol. 62, pp. 2316–2324, 2014. [Online]. Available: <http://dx.doi.org/10.1109/TMTT.2014.2345352>
- [7] R. Amirkhazadeh, H. Sjoland, J.-M. Redoute, D. Nobbe, M. Faulkner, “High-resolution passive phase shifters for adaptive duplexing applications in SOS process”, *IEEE Trans. On Microwave Theory and Techniques*, vol. 62, pp. 1678–1685, 2014. [Online]. Available: <http://dx.doi.org/10.1109/TMTT.2014.2327980>
- [8] E. Metlevskis, R. Martavicius, “Computer models of meander slow-wave systems with additional shields”, *Elektronika ir elektrotechnika*, no. 3, pp. 61–64, 2012.
- [9] V. Urbanavicius, A. Gurskas, R. Martavicius, “Simulation of the meander delay line using the hybrid method”, *Elektronika ir elektrotechnika*, no. 2, pp. 6–9, 2009.
- [10] S. Ibrahim, G. Szczepkowski, R. Farell, “The effect of impedance mismatch on phase linearity of GCPW loaded transmission lines and shunt stubs”, in *Proc. 25th IET Irish Signals & Systems Conf. 2014 and 2014 China-Ireland Int. Conf. Information and Communications Technologies (ISSC 2014/CICT 2014)*, Limerick, 2014, pp. 392–395.
- [11] Y. Tian, K. Lee, H. Wang, “A 390 ps on-wafer true-time-delay line developed by a novel micro-coax technology”, *IEEE Microwave and Wireless Components Letters*, vol. 24, pp. 233–235, 2014. [Online]. Available: <http://dx.doi.org/10.1109/LMWC.2013.2296294>
- [12] X. Lan, M. Kintis, C. Hansen, W. Chan, G. Tseng, M. Tan, “A simple DC to 110 GHz MMIC true time delay line”, *IEEE Microwave and Wireless Components Letters*, vol. 22, pp. 369–371, 2012. [Online]. Available: <http://dx.doi.org/10.1109/LMWC.2012.2200099>
- [13] S. P. Natarajan, A. M. Hoff, T. M. Weller, “Polyimide core 3D rectangular micro coaxial transmission lines”, *Microwave and Optical Technology Letters*, vol. 52, pp. 1291–1293, 2010. [Online]. Available: <http://dx.doi.org/10.1002/mop.25212>
- [14] S. Staras, A. Katkevicius, “Properties of helical structures containing periodical inhomogeneities”, *Elektronika ir elektrotechnika*, no. 3, pp. 49–52, 2010.
- [15] R. K. Mongia, I. J. Bahl, P. Bhartia, J. Hong, *RF and Microwave Coupled-Line Circuits*. 2nd Ed. Artech House, Inc., 2007, pp. 17–51.
- [16] S. Staras, R. Martavicius, J. Skudutis, V. Urbanavicius, V. Daskevicius, *Wide-Band Slow-Wave System. Simulation and Application*. CRC Press, Boca Raton: Taylor & Francis Group, 2012, pp. 72–86.